BMCL Digest

Optimisation of 6-substituted isoquinolin-1-amine based ROCK-I inhibitors

Peter Ray *, Jane Wright, Julia Adam, Sylviane Boucharens, Darcey Black, Angus R. Brown, Ola Epemolu, Dan Fletcher, Margaret Huggett, Phil Jones, Steven Laats, Amanda Lyons, Jos de Man, Richard Morphy, Brad Sherborne, Lorcan Sherry, Nicole van Straten, Paul Westwood, Mark York

Discovery Research, MSD, Newhouse, Lanarkshire, ML1 5SH Scotland, UK

ABSTRACT

Rho kinase is an important target implicated in a variety of cardiovascular diseases. Herein, we report the optimisation of the fragment derived ATP-competitive ROCK inhibitors **1** and **2** into lead compound **14A**. The initial goal of improving ROCK-I potency relative to **1**, whilst maintaining a good PK profile, was achieved through removal of the aminoisoquinoline basic centre. Lead **14A** was equipotent against both ROCK-I and ROCK-II, showed good in vivo efficacy in the spontaneous hypertensive rat model, and was further optimised to demonstrate the scope for improving selectivity over PKA versus hydroxy Fasudil **3**.

© 2010 Elsevier Ltd. All rights reserved.

Rho kinase (ROCK) belongs to the AGC family of serine/threonine kinases and interacts with the GTP-binding protein RhoA to afford active protein. Two iso-forms of Rho kinase have been described (ROCK-I and ROCK-II) and they share high homology in the ATP binding site. RhoA and its downstream kinase (ROCK) have been implicated in a number of important roles such as regulation of smooth muscle contraction, cytoskeleton rearrangement, cell migration and proliferation. Furthermore, a large amount of pre-clinical research effort with various inhibitors has demonstrated that both RhoA and ROCK are important targets for several cardiovascular diseases.[1]

Acute clinical studies with Fasudil, which is presumed to act via its active metabolite hydroxyl Fasudil **3**, have demonstrated efficacy and safety in treating cerebral vasospasm, ischemic stroke and stable angina. Fasudil has also shown beneficial effects in a number of other cardiovascular diseases, including angina pectoris, hypertension, coronary vasospasm, restenosis after percutaneous coronary intervention and arteriosclerosis.[2] Recently, there has been a surge in the research effort towards identifying potent and selective ROCK inhibitors.[3]

Previously, we reported the ROCK-I inhibitor **1**, which was obtained from fragment based approach. Compound **1** has similar ROCK-I affinity, potency and cell based efficacy (which provides an in vitro understanding of MCP-1-induced migration of monocytes in unstable atherosclerotic lesions) to hydroxy Fasudil **3**.

However, it has superior in vivo pharmacokinetics in the C57 mouse. Although derivative **2** demonstrated the scope to improve affinity, potency and cell based efficacy, it suffered for poor in vivo bioavailability and also had a high clearance and volume in the rat (Table 1).[4]
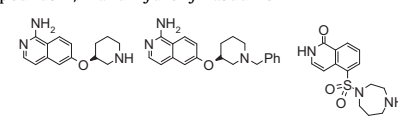
Herein, we report on the optimisation of compounds **1** and **2**. The optimisation goal was to increase the potency of **1**, whilst maintaining the good pharmacokinetic properties. Compound **1** has poor Caco-2 permeability, however, it has excellent bioavailability and it was rationalized that this small dibasic compound was absorbed predominantly via the para-cellular route. The Caco-2 permeability for **2** was worse, despite the increased $c \log P/\log D$. Furthermore, **2** suffered from poor bioavailability and it was rationalized that the dibasic nature of this larger compound was problematic for absorption,[5] as it could not be absorbed via the para-cellular route.

An initial effort was made to reduce the pK_a of the piperidine amine **1** through alkylations with suitable electron withdrawing derivatives. However, the resultant compounds had both poor ROCK-1 potency and microsomal stability. A further attempt was also made to lower the lipophilicity of the benzyl derivative in **2**, by changing the phenyl to various heterocycles. However, Caco-2 permeability remained an issue and only moderate to poor liver microsomal stabilities were obtained (data not shown).

Since the aminoisoquinoline core is reported to have a pK_a of ~7.5,[6] subsequent optimisation focused on analogues of isoquinoline with differing substituents at the 1-position that would significantly alter the pK_a. Isoquinoline itself was a very interesting

* Corresponding author. Tel.: +44 (0)1698 736127.
 E-mail address: p.ray@btinternet.com (P. Ray).

Table 1
ROCK-I hit compounds **1**, **2** and hydroxy Fasudil **3**

	1[a]	**2**[a]	**3**[a]
ROCK-I pK_i	7.43 ± 0.08	nd	7.46 ± 0.13
ROCK-I IMAP pIC$_{50}$	5.67 ± 0.16	6.62 ± 0.01	6.12 ± 0.02
ROCK-II IMAP pIC$_{50}$	5.95 ± 0.04	7.04 ± 0.09	6.24 ± 0.06
THP migration pIC$_{50}$	5.30 ± 0.28	6.11 ± 0.21	5.16 ± 0.31
Caco-2 (5×10^{-6} cm/s)	6.3	2.2	nd
A–B/B–A	3.6	1.5	
	C57 Mouse	Wistar Rat	C57 Mouse
Bioavailability ($F\%$)	>75	7	57
Cl$_p$ (mL/min/kg)	9.5	295	34
V_{ss} (L/kg)	11	8.2	2.4
$T_{1/2}$ (h)	5.8	8.2	0.75

[a] pIC$_{50}$ values are shown as mean ± standard deviation from $n = 2$–5 separate experiments (except where $n = 1$).
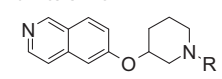
analogue and this was obtained by demethylation of **6** to afford the phenol, followed by a Mitsunobu coupling with *N*-boc-3-hydroxy-piperidine to give **7**. TFA deprotection afforded isoquinoline **8A**, which could be converted to the *N*-benzyl derivative by reductive alkylation with benzaldehyde, and then resolved to afford the single enantiomers **8B** and **8C** (Scheme 1).

Isoquinoline **8A** showed ROCK-1 activity comparable to **1** and enantiomers **8B** and **8C** showed improved potency (Table 2). Compound **8B** was profiled in vivo and showed improved bioavailability with respect to **2**. However, the pharmacokinetic profile of **8B** was still not optimal, as it was associated with a high clearance and high volume of distribution in the rat. Furthermore, **8B** showed potent 2D6 and 3A4 cytochrome P450 inhibition (Table 4).

The above data supported the rationale for further modification of the pK_a in order to improve the pharmacokinetics. Hence, our attention shifted onto the isoquinolin-1-one building block **9**, which was synthesized as shown in Scheme 2. Homologation of 3-methoxybenzaldehyde **10** afforded acid **11**, which was reacted with diphenylphosphoryl azide and then heated to temperatures in excess of 250 °C to afford isoquinolin-1-one **12**. Deprotection of **12** with BBr$_3$ afforded phenol **9**. With **9** in hand, S_N2 PS-BEMP mediated displacement of the readily prepared mesylates of *N*-Boc-protected aminoalcohols afforded ethers **13A–G**. *N*-Boc deprotection of **13A–G** afforded compounds **14A–G**.
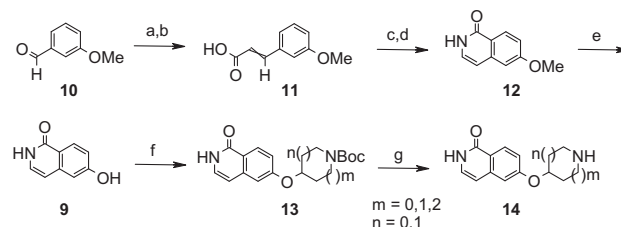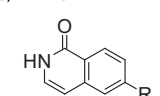
Gratifyingly, *S*-isomer **14A** had an ROCK-I pIC$_{50}$ of 7.21 ± 0.22 (Table 3). The *R*-isomer **14B** and the 4-substituted piperidine **14C** were both less potent. However, the azepine **14D** also showed good ROCK-I potency with its enantiomer **14E** being less potent. The pyrrolidines **14F** and **14G** showed moderate potencies.
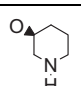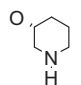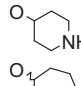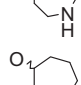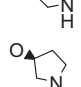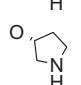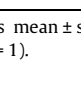
Compound **14A** was selected for further profiling and was found to have potent ROCK-I affinity as well as similar potency in the ROCK-II IMAP assay as ROCK-I (Table 4). It showed improved potency in the THP migration assay relative to hydroxyl Fasudil **3** and no major inhibition of any of the CYP isoforms studied. Due to the slow rate of metabolism, the enzymes responsible for any metabolism of **14A** could not be identified. Rat and human plasma
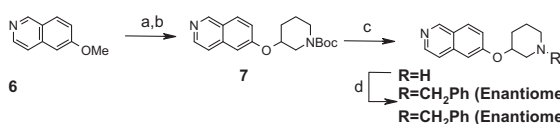
Table 2
ROCK-I IMAP SAR for isoquinolines **8A–C**

Compounds	R	ROCK-I (IMAP) pIC$_{50}$[a]
8A	*rac*-H	5.75 ± 0.02
8B	*S*-Bn	6.77 ± 0.04
8C	*R*-Bn	7.14 ± 0.02

[a] pIC$_{50}$ values are shown as mean ± standard deviation from $n = 2$–5 separate experiments (except where $n = 1$).

Scheme 2. Reagents and conditions: (a) Ph$_3$PCHCO$_2$Me, toluene; (b) NaOH; (c) DPPA, NEt$_3$, toluene; (d) diphenylmethane, >250 °C; (e) BBr$_3$, DCM or HCl; (f) PS-BEMP, MeCN, 160 °C; (g) TFA, DCM.

Table 3
ROCK-I IMAP SAR for R^2 amines, **14A–G**

Compounds	R	ROCK-I (IMAP) pIC$_{50}$[a]
14A		7.21 ± 0.22
14B		6.17 ± 0.04
14C		6.73 ± 0.10
14D		7.24 ± 0.07
14E		6.48 ± 0.11
14F		6.28 ± 0.10
14G		6.06 ± 0.16

[a] pIC$_{50}$ values are shown as mean ± standard deviation from $n = 2$–5 separate experiments (except where $n = 1$).

protein binding for **14A** were 20% and 6%, respectively. This low level of binding across species indicates that most of the drug in the plasma will be available for effect. The pharmacokinetic studies for **14A** in rat show suitable oral bioavailability. Furthermore, both distribution volume and clearance are moderate, resulting in a suitable half life. The estimated fraction of the dose absorbed was 62% which is consistent with its high solubility, low molecular
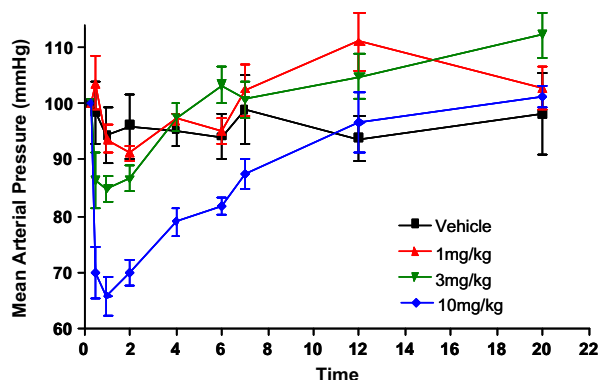
Scheme 1. Reagents and conditions: (a) BBr$_3$, DCM, −78 °C to 20 °C; (b) *N*-boc-3-hydroxypiperidine, DEAD, PPh$_3$, THF, 20 °C; (c) TFA, DCM.

Table 4
Profiling of compounds **8B** and **14A**

	8B[a]	**14A**[a]
ROCK-I pK_i	nd	8.6
ROCK-I IMAP pIC$_{50}$	6.77 ± 0.04	7.21 ± 0.22
ROCK-II IMAP pIC$_{50}$	7.10 ± 0.08	7.41 ± 0.07
THP migration pIC$_{50}$	6.48 ± 0.01	6.18 ± 0.16
H/R/M liver micr: Cl$_{int}$, μL/mL/mg	nd	<12, 24, 17
R/H Heps:Cl$_{int}$, mL/mL/1 × 10^6 cells	21/nd	<6/2
Caco-2 (×10^{-6} cm/s) A–B/B–A	11.6/17.6	14.3/11.2
2C19, 3A4, 1A2, 2D6, 2C9	3A4, 2D6 <1 μM	All
Cyp inhibition	& rest >5 μM	>5 μM
hERG (Dofetilide) pK_i	5.7	<4
Wistar rat	rat	rat
Bioavailability (*F*%)	37	31
Clp (mL/min/kg)	184	42
V_{ss} (L/kg)	8.9	8.2
$T_{1/2}$ (h)	0.85	1.75

[a] pIC$_{50}$ values are shown as mean ± standard deviation from n = 2–5 separate experiments (except where n = 1).

Figure 1. The effect of **14A** on mean arterial pressure (MAP) in the SHR model.

Table 5
Full dose response data for **14A** and hydroxy Fasudil **3**

Kinase	Assay format	pIC$_{50}$	
		14A	3
PKCδ (h)	RFBA	6.5	4.6
PKCη (h)	RFBA	6.4	4.7
PKCμ (h)	RFBA	6.3	5.0
PrkX (h)	RFBA	7.1	5.2
PKA	RFBA	6.5	5.0
ROCK-I	RFBA	6.6	5.5
ROCK-I	IMAP[a]	7.21 ± 0.22	6.12 ± 0.02

[a] pIC$_{50}$ values are shown as mean ± standard deviation from n = 2–5 separate experiments (except where n = 1).

weight and permeability in the Caco-2 assay. Hence, the strategy to modulate one of the basic centers was successful in affording a

potent ROCK-I inhibitor with improved permeability and a suitable pharmacokinetic profile.

Compound **14A** was evaluated in the NovaScreen general side effect panel of 64 assays at 10 μM and only showed limited binding to the serotonin and dopamine transporters (56% and 43%, respectively). Compound **14A** showed limited hERG binding affinity in the [3*H*]-dofetilide binding assay, with a pK_i <4, and produced <20% inhibition of hERG tail current in a high throughput electrophysiology assay at 10 μM. Compound **14A** showed no activity in the Vitotox assay in the presence or absence of S9 liver extract and did not activate the human pregnane X receptor (PXR) or the aryl hydrocarbon receptor (AhR).

In vivo, **14A** reduced blood pressure (BP) in the spontaneous hypertensive rat model by 34% at 10 mg/kg and 15% at 3 mg/kg po (Fig. 1). The effect was greater than that observed for the reference standard Y-27632.[7]
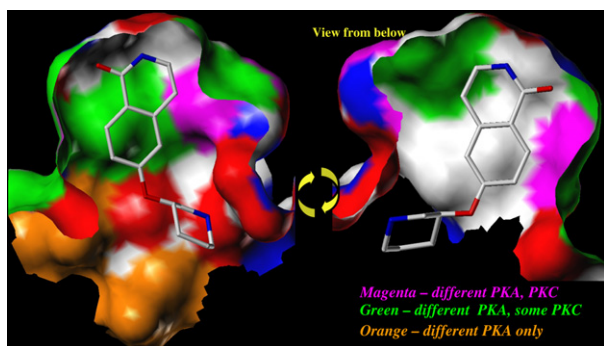
The full kinase selectivity profiles for hydroxy Fasudil **3** (at 10 μM) and **14A** (at 1 μM) were obtained from Millipore. The profile for **14A** compares well with that of hydroxy Fasudil **3**. Compound **14A** appeared to be less selective than hydroxy Fasudil **3** for the AGC-related kinases [in particular PKA, PKC (δ, η, μ) and PrkX]. Overall, **14A** was highly selective over the panel of kinases tested, with selectivity of >25-fold over >92% of the non-AGC family kinases tested. It is known that Fasudil, and its more potent, active metabolite hydroxy Fasudil **3**, are efficacious in man with no apparent side effects up to 80 mg/kg t.i.d (po) for 8 weeks.[8] Thus, a selectivity profile which is equivalent or better than that of hydroxy Fasudil **3** is believed to be a desirable goal. Further full dose response profiling confirmed that **14A** was less selective for PKC & PKA isoforms compared to hydroxy Fasudil **3** (Table 5).

Using a homology model for ROCK-I, developed initially using PKA as a template and then modified according to the published ROCK-I crystal structures, docking studies with known ligands and lead **14A** provided suggestions for isoquinolone series modifications.[9] Compound **14A** appears tightly bound in the ATP binding pocket making interactions through the adenosine and ribose binding regions with limited exploration of space not occupied by ATP. The model was then used to identify residues available for interactions with **14A**. The sequence differences between ROCK-I, PKA and the PKC isoforms were defined (Table 6) and mapped onto the ROCK-I homology model (Fig. 2). The computational modeling data suggested a focus on interactions with residues I82, M128 and A215. The appropriate areas of space relative to the proposed binding mode for **14A** are highlighted in magenta in the Figure 2. Additional areas highlighted are those in: Green, which might afford PKA and some PKC subtype selectivity (F368, L205 and M153). Orange, those which would only afford selectivity over PKA (D160, D202).

From analysis of the selectivity data from the literature, it was clear that selectivity over PKA was a key issue for optimisation. It was hypothesized that focusing on improving selectivity over PKA would afford compounds with an overall improved selectivity profile. Initial full dose response PKA profiling of **14A**, **14C** and **14D**

Table 6
ATP site residue for closely related AGC kinase

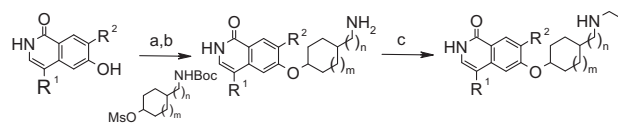| Res. No.	Rock	PKCdelta	PKCeta	PKCmu	PKCepsilon	PKCiota	PKCbeta	PKCgamma	PKCzeta	PKA (h)
82	I	L	L	L	L	I	L	L	I	L
128	M	L	L	L	L	F	L	L	F	L
153	M	M	M	M	M	I	M	M	I	M
160	D	D	D	D	D	D	D	D	D	E
202	D	D	D	E	D	D	D	D	D	E
205	L	L	L	L	L	L	M	M	L	L
215	A	A	A	C	A	T	A	T	T	T
368	F	F	F	Y	F	F	F	F	F	F

Figure 2. Sequence differences between ROCK-I, PKA and the PKC isoforms mapped onto the ROCK-I homology model. Magenta areas might afford PKA and PKC subtype selectivity. Green areas might afford PKA and some PKC subtype selectivity. Orange area might afford selectivity over PKA.

suggested that changing the ring size had little effect on selectivity over PKA (Table 7). In order to probe the green and magenta residue differences for PKA within Figure 2, derivatives **15A** and **15B** were prepared using equivalent synthetic methodology to that described in Scheme 2. Compound **15A** showed a decrease in both

Table 7
ROCK-I IMAP and PKA RFBA pIC$_{50}$ data, **14A,C,D, 15A,B** and **16A–E**

Compd	R^1	R^2	R^3	PKA RFBA pIC$_{50}$	ROCK-I IMAP pIC$_{50}$[a]	ROCK-I minus PKA
14A	H	H	(O-piperidine, N-H)	6.5	7.21 ± 0.22	0.7
14C	H	H	(O-piperidine, NH)	5.8	6.73 ± 0.10	0.9
14D	H	H	(O-azepane, N-H)	6.4	7.24 ± 0.07	0.8
15A	Me	H	(O-piperidine, N-H)	5.6	6.23 ± 0.05	0.6
15B	H	Me	(O-piperidine, N-H)	6.3	7.32 ± 0.04	1
16A	H	H	(O-cyclopentyl, NH$_2$)	5.2	6.64 ± 0.06	1.4
16B	H	H	(O-cyclohexyl, NH$_2$)	6.2	7.50 ± 0.14	1.3
16C	H	H	(O-cyclohexyl, NHEt)	5.1	6.92 ± 0.09	1.8
16D	H	H	(O-cyclopentyl, NH$_2$)	5.5	7.09 ± 0.06	1.6
16E	H	H	(O-cyclopentyl, NH$_2$)	5.2	6.78 ± 0.03	1.6

[a] pIC$_{50}$ values are shown as mean ± standard deviation from $n = 2$–5 separate experiments (except where $n = 1$).

Scheme 3. Reagents and conditions: (a) PS-BEMP, MeCN, 160 °C; (b) TFA, DCM; (c) acetaldehyde, MeCN, AcOH, NaBH(OAc)$_3$.

ROCK-1 and PKA potency. However, **15B** maintained a similar ROCK-I potency and afforded a slightly improved selectivity over PKA (Table 7).

The next optimisation cycle involved making changes to the amine scaffold within the orange residue differences for PKA within Figure 2. Amines, **16A–E**, were readily prepared according to Scheme 3. Compound **16A** lost potency at both ROCK-1 and PKA, however, improved selectivity over PKA was obtained. The cyclohexyl derivative **16B** retained ROCK-1 potency and the selectivity over PKA was improved. Furthermore, reductive amination of **16B** afforded **16C**, which had suitable ROCK-I potency and good selectivity over PKA. Further homologated amines such as **16D** and **16E** were also prepared and both showed promising ROCK-I potencies and improved selectivity over PKA versus the lead **14A** (Table 7).

In conclusion, the fragment derived aminoisoquinolines **1** and **2**, were optimised into isoquinolone lead **14A** through a strategy of removing the aminoisoquinoline basic centre. Compound **14A** is ~10-fold more potent than hydroxy Fasudil **3** and is highly selective in a large panel of receptor and enzyme targets. In vitro, **14A** demonstrated concentration-dependent inhibition of MCP-1 stimulated chemotaxis. In vivo, **14A** lowered blood pressure in the spontaneous hypertensive rat model of arterial hypertension and the antihypertensive effect was superior to that of the first generation reference compound Y-27632. Full dose response kinase profiling revealed that selectivity over PKA was an issue and further optimisation provided compounds which demonstrate the scope for improving selectivity over PKA.

References and notes

1. Amano, M.; Fukata, Y.; Kaibuchi, K. *Exp. Cell Res.* **2000**, *261*, 44; Shimokawa, H.; Morishige, K.; Miyata, K.; Kandabashi, T.; Eto, Y.; Ikegaki, I.; Asano, T.; Kaibuchi, K.; Takeshita, A. *Cardiovasc. Res.* **2001**, *51*, 169; Morishige, K.; Shimokawa, H.; Eto, Y.; Kandabashi, T.; Miyata, K.; Matsumoto, Y.; Hoshijima, M.; Kaibuchi, K.; Takeshita, A. *Arterioscler. Thromb. Vasc. Biol.* **2001**, *21*, 548; Saito, H.; Minamiya, Y.; Saito, S.; Ogawa, J. *J. Leukocyte Biol.* **2002**, *72*, 829; Kawano, Y.; Yoshimura, T.; Kaibuchi, K. *J. Med. Sci.* **2002**, *65*, 1; Seasholtz, T. M. *Am J Physiol Cell Physiol.* **2003**, *284*, C596; Lee, D. L.; Webb, R. C.; Jin, L. *Hypertension* **2004**, *44*, 796; Schwartz, M. *J. Cell Sci.* **2004**, *117*, 5457; Budzyn, K.; Marley, P. D.; Sobey, C. G.; Irooka, Y.; Shimokawa, H.; Takeshita, A. *Drug News Perspect.* **2004**, *17*, 523–527; Seasholtz, T. M.; Brown, J. H. *Mol. Interv.* **2004**, *4*, 348; Lai, A.; Frishman, W. H. *Cardiol. Rev.* **2005**, *13*, 285; Budzyn, K.; Marley, P. D.; Sobey, C. G. *Trends Pharmacol. Sci.* **2006**, *27*, 97; Shi, J.; Wei, L. *Arch. Immunol. Ther Exp.* **2007**, *55*, 61.
2. Mueller, B. K.; Mack, H.; Teusch, N. *Nat. Rev. Drug Disc.* **2005**, *4*, 387.
3. Hu, E.; Lee, D. *Expert Opin. Ther. Targets* **2005**, *9*, 4; Stavenger, R. A.; Cui, H.; Dowdell, S. E.; Franz, R. G.; Gaitanopoulos, D. E.; Goodman, K. B.; Hilfiker, M. A.; Ivy, R. L.; Leber, J. D.; Marino, J. P., Jr.; Oh, H.-J.; Viet, A. Q.; Xu, W.; Ye, G.; Zhang, D.; Zhao, Y.; Jolivette, L. J.; Head, M. S.; Semus, S. F.; Elkins, P. A.; Kirkpatrick, R. B.; Dul, E.; Khandekar, S. S.; Yi, T.; Jung, D. K.; Wright, L. L.; Smith, G. K.; Behm, D. J.; Doe, C. P.; Bentley, R.; Chen, Z. X.; Hu, E.; Lee, D. *J. Med. Chem.* **2007**, *50*, 2; Goodman, K. B.; Cui, H.; Dowdell, S. E.; Gaitanopoulos, D. E.; Ivy, R. L.; Sehon, C. A.; Stavenger, R. A.; Wang, G. Z.; Viet, A. Q.; Xu, W.; Ye, G.; Semus, S. F.; Evans, C.; Fries, H. E.; Jolivette, L. J.; Kirkpatrick, R. B.; Dul, E.; Khandekar, S. S.; Yi, T.; Jung, D. K.; Wright, L. L.; Smith, G. K.; Behm, D. J.; Bentley, R.; Doe, C. P.; Hu, E.; Lee, D. *J. Med. Chem* **2007**, *50*, 6.
4. Ray, P.; Wright, J.; Adam, J.; Boucharens, S.; Black, D.; Brown, A. R.; Epemolu, O.; Fletcher, D.; Huggett, M.; Laats, S.; Lyons, A.; Man, J. de; Morphy, R.; Sherborne, B.; Sherry, L.; Straten, N. v.; Westwood, P. *Bioorg. Med. Chem. Lett.* **2011**, *21*, 97.
5. Denonne, F.; Atienzar, F.; Célanire, S.; Christophe, B.; Delannois, F.; Delaunoy1, F.; Delporte, M.-L.; Durieu1, V.; Gillard, M.; Lallemand1, B.; Lamberty, Y.; Lorent, G.; Vanbellinghen1, A.; Houtvin, N.; Verbois, V.; Provins, L. *ChemMedChem* **2010**, *5*, 206.
6. Trujillo, J. I.; Huang, H.-C.; Neumann, W. L.; Mahoney, M. W.; Long, S.; Huang, W.; Garland, D. J.; Kusturin, C.; Abbas, Z.; South, M. S.; Reitz, D. B. *Bioorg. Med. Chem. Lett.* **2007**, *17*, 4568; Takami, A.; Iwakubo, M.; Okada, Y.; Kawata, T.; Odai, H.; Takahashi, N.; Shindo, K.; Kimura, K.; Tagami, Y.; Miyake, M.; Fukushima, K.;

Inagaki, M.; Amano, M.; Kaibuchi, K.; Iijima, H. *Bioorg. Med. Chem.* **2004**, *12*, 2115.

7. Uehata, M.; Ishizaki, T.; Satoh, H.; Ono, T.; Kawahara, T.; Morishita, T.; Tamakawa, H.; Yamagami, K.; Inui, J.; Maekawa, M.; Narumiya, S. *Nature* **1997**, *389*, 990.

8. Vicari, R. M.; Chaitman, B.; Keefe, D.; Smith, W. B.; Chrysant, S. G.; Tonkon, M. J.; Bittar, N.; Weiss, R. J.; Morales-Ballejo, H.; Thadani, U. *J. Am. Coll. Cardiol.* **2005**, *46*, 1803.

9. Takami, A.; Iwakubo, M.; Okada, Y.; Kawata, T.; Odai, H.; Takahashi, N.; Shindo, K.; Kimura, K.; Tagami, Y.; Miyake, M.; Fukushima, K.; Inagaki, M.; Amano, M.; Kaibuchi, K.; Iijima, H. *Bioorg. Med. Chem.* **2004**, *12*, 2115. The study was conducted in 2004. A ROCK crystal structure was published in 2006.; Jacobs, M.; Hayakawa, K.; Swenson, L.; Bellon, S.; Fleming, M.; Taslimi, P.; Doran, J. *J. Biol. Chem.* **2006**, *281*, 260; Furthermore, ROCK inhibitors bound to PKA were also reported. Breitenlechner, C.; Gassel, M.; Hidaka, H.; Kinzel, V.; Huber, R.; Engh, R. A. *Bossemeyer. Structure.* **2003**, *11*, 1595.